Materials Research Innovations

ISSN: 1432-8917 (Print) 1433-075X (Online) Journal homepage: https://www.tandfonline.com/loi/ymri20

Preparation of thermal infrared and microwave absorber using $WO_3/MnFe_3O_4$/polyaniline nanocomposites

Mahdi Boujar Dolabi, Ali Azimi & Seyed Hossein Hosseini

To cite this article: Mahdi Boujar Dolabi, Ali Azimi & Seyed Hossein Hosseini (2019): Preparation of thermal infrared and microwave absorber using $WO_3/MnFe_3O_4$/polyaniline nanocomposites, Materials Research Innovations, DOI: 10.1080/14328917.2019.1677078

To link to this article: https://doi.org/10.1080/14328917.2019.1677078

Published online: 18 Oct 2019.

MATERIALS RESEARCH INNOVATIONS
https://doi.org/10.1080/14328917.2019.1677078

Taylor & Francis
Taylor & Francis Group

Preparation of thermal infrared and microwave absorber using $WO_3/MnFe_3O_4$/polyaniline nanocomposites

Mahdi Boujar Dolabi[a], Ali Azimi[b] and Seyed Hossein Hosseini[c]

[a]Department of Chemistry, Payame Noor University, Tehran, Iran; [b]Department of Chemistry, Faculty of Science,East Tehran Branch, Islamic Azad University, Tehren, Iran; [c]Department of Chemistry, Faculty of Science, Central Tehran Branch, Islamic Azad University, Tehran, Iran

ABSTRACT

In this study tungsten trioxide has been synthesised as a thermal infrared (TIR) absorbent by sol–gel method and characterised by X-ray diffraction (XRD), field emission scanning electron microscopes (FESEM) and transmission electron microscopy (TEM). XRD analysis shows that the single phase and hexagonal tungstate was prepared. The crystallite size measured by Scherer formula is in good accordance with the crystallite nano size measured by TEM. The polyaniline (PANI) was coated on $WO_3/MnFe_2O_3$ nanoparticles (NPs, 50/50 wt%) via in situ polymerisation by core-shell structure $WO_3/MnFe_2O_3$/PANI nanocomposite (50% wt as core). Structural and morphological characteristics of the produced nanocomposite were studied via X-ray diffraction, Fourier transformation infrared spectroscopy and scanning electron microscopy. The electric property was also performed by four probe method. The results showed that the $WO_3/MnFe_2O_3$/PANI nanocomposites have good electric property. The TIR absorption of nanocomposite was investigated at 10–40 µm frequencies. The TIR images testing showed that the ability of infrared thermal imaging was increased by increasing $WO_3/MnFe_2O_3$ as core and independent to increasing PANI as final shell. The test microwave absorption properties of the nanoparticles powder dispersing in PANI and thickness of 1.5 mm were investigated by using a vector network analysers in the frequency range of 8–12 GHz. A minimum reflection loss of the nanocomposite reaches -12 dB were observed at 8.8 and 11.6 GHz, respectively.

ARTICLE HISTORY
Received 8 July 2019
Accepted 1 October 2019

KEYWORDS
Thermal infrared absorbent; microwave absorber; polyaniline; tungsten trioxide nanoparticles; Conducting polymers; Nanocomposite; Nanoparticle

Introduction

Tungsten oxide WO_3 is an *n*-type semiconductor with interesting physical and chemical properties that make it suitable for various technological applications such as catalyst, electro chromic and gas sensors [1]. At present, materials scientists have already prepared WO_3 with different shape. Wu et al. [2] prepared homogeneous nano-WO_3 grains using gas–liquid reaction. Santos et al. [3] synthesised WO_3 nanoparticles (NPs) for biosensing applications. Cheng et al. [4] fabricated WO_3 nanotubes using template. The WO_3 nanoparticles (NPs) were prepared by Pandey with electrical properties [5]. Doped WO_3 for photocatalytic water or WO_3 mixed with other metals exhibits various properties, different types of morphologies and has many applications [6]. WO_3 NPs and nanocrystalline thin films have a wide range of applications in non-toxic to stem cells and cancer cells [7]. Manganese ferrite is one of importance magnetics materials that was used as bioapplications of magnetic nanoparticles [8], ionic liquids affords [9] and absorbing materials [10].

Polyaniline (PANI) is the intrinsic conducting polymer which offers very promising opportunities for industrial applications [11]. PANI assisted by both oxidation and protonation processes, it is the only conducting polymer whose electronic structure can be controlled in a reversible manner. Several nanostructures of PANI such as nanofibers [12], nanotubes [13] and nanoclaster [14] have been prepared by different of synthesis methods. It is can be used as sensors [13,15] and electromagnetic absorbers [16,17].

The thermal infrared (TIR) radiation refers to electromagnetic waves with a wavelength of between 5 and 40 micrometres. Most remote sensing applications make use of the 8–13 micrometre range. The main difference between TIR and the other infrared (IR) regions discussed is that TIR is emitted energy that is sensed digitally, whereas the near IR 'photographic IR' is reflected energy that causes a chemical reaction in film emulsion. The electromagnetic interference (EMI) and electromagnetic radiation (EMR) are becoming a serious problem due to expanding use of wireless devices and high frequency operated circuit devices in gigahertz range. The various studies on microwave absorption properties of various materials have been investigated to select the suitable material to cope up with the problems related EMI [18], and so on as microwave absorbing materials [19,20]. $BaTiO_3$ and $BaFe_{12}O_{19}$ exhibit various electrical and magnetic properties of which the complex permeability and the complex permittivity, in particular, are important in determining their high frequency characteristics. So, IR and microwave absorbing properties of $BaTiO_3$/polyaniline and $BaFe_{12}O_{19}$/polyaniline composites were investigated by Wu, too [21]. The preceding works, we have published some papers about TIR absorbing materials [22,23] based conducting polymers and NPs. In this paper, WO_3 nanoparticles were prepared by reacting tungstic acid with hydrogen peroxide and the presence of polyethylene

CONTACT Seyed Hossein Hosseini dr.shhosseini@gmail.com, shhosseini@iiau.ac.ir Department of Chemistry, Faculty of Science, Central Tehran Branch, Islamic Azad University, Tehran, Iran

Research Novelties
Preparation of $WO_3/MnFe_3O_4$/polyaniline nanocomposites.The $WO_3/MnFe_3O_4$/polyaniline nanocomposites have shielding structures into thermal IR and microwave.

glycol (PEG) as a template. Then its nanocomposites with PANI were synthesised in different weight ratios and thicknesses as TIR absorbent that exhibit high IR absorptivity. The results from TIR absorption can be used to interpret the electromagnetic properties and military applications.

Experimental

Materials and methods

All the reagents used in this experiment such as tungstic (VI)acid, dodecylbenzenesulfonic acid (DBSA), ammonia persulphate (APS), hexamethylene tetraamine (HMTA), ethylene glycol (EG), polystyrene, $FeCl_2$, $MnCl_2$ and potassium nitrate were obtained from Merck. Poly ethylene glycol (PEG, molecular weight of 300) and hydrogen peroxide (30–32%, grade AR) were obtained from Fluka and OReC. Other chemicals were of analytical grade and used without further purification. Distilled and deionised water was used throughout the work. Aniline monomer (analytical grade, Merck) was distilled twice under reduced pressure and stored below 0°C.

The ultrasonic experiments were carried out by an ultrasonic disperser (BANDELIN sonorex digitec, 35 kHz, Germany). The XRD patterns of the samples were collected on a Philips-PW1800 with Cu Kα radiation (λ = 1.54184Å) in the 2θ = 4-90° with steps of 0.02°, scanning operated at 40 kV and 30 mA (Netherland). Field emission scanning electron microscopes (FESEM) were performed by Hitachi S-4160 model (Japan) to observe the surface morphologies of the NPs. The morphologies of as prepared samples were examined with transmission electron microscopy (TEM) by ZWISS-EM900, Germany. Samples of TEM were prepared by dispersing the final NPs in ethanol; the suspension was then dropped on copper grids. The magnetic measurements were carried out at room temperature using a IRI-Kashan vibrating sample magnetometer (VSM) with a maximum magnetic field of 10 kOe (Research Institute NanoTechnology of Kashan-Iran). Microwave absorption properties of nanocomposites were measured by using microwave vector network analyser (Agilent technologies Inc.8722-USA) in the 8–12 GHz range at room temperature. The electrical conductivity of compressed pellets of polymers and nanocomposites was measured using a standard four-probe set-up connected to a Keithley system comprising a voltmeter and a constant high-current source, made in IRAN. The TIR absorption properties of the nanocomposites were measured by Thermal camera (SATIR-G96 (Irland), -20 to +250 °C).

Synthesis of WO_3 nanocrystalline powders

WO_3 nanocrystalline powders have been obtained by a soft chemistry route based on tungstic acid. Tungstic acid was dissolved in a 50:50 volume mixture of methanol and water with tungsten over water molar ratio of 25. This solution was heated at 80°C for 24 h under stirring in air and dried by further heating at 110°C in air, leading to tungsten oxide hydrate. The precipitation has been dried at 220°C. This material was annealed in a furnace between 700°C for 3 h to obtain nanocrystalline WO_3.

Preparation of $MnFe_2O_4$ nanoparticles

In a typical preparation process, 2 mL polystyrene colloid solution was diluted with 250 mL deoxygenated distilled water and then mixed with the metal salts solution, which contained 10 mmol $FeCl_2$ and 5 mmol $MnCl_2$. After dispersed under ultrasonic for several minutes, the mixture was in corporate with 4 g HMTA and 0.5 g potassium nitrate and heated to 85°C under gentle stirring. After 3 h, the system was cooled to room temperature. The solution was poured in to excess distilled water, then magnetic particles were deposited using magnetic field. The precipitate was washed with distilled water for several times and then dried in oven at 80° C for 24 h. In addition, to modify the surface chemical properties of the composites magnetic spheres, 5 mL ethylene glycol (EG) was added into the reaction solution before the incorporation of HMTA.

Preparation of $WO_3/MnFe_2O_4$/PANI nanocomposites

The 1 g DBSA was dissolved in distilled water with vigorous stirring for about 20 min. The $WO_3/MnFe_2O_4$ NPs (1:1 wt) were added to the DBSA solution under stirring condition for approximately 1/2 h. Then 1 mL of doubly distilled aniline as monomer was added to the suspension and stirred for 30 min. The $WO_3/MnFe_2O_4$ (50/50 weight ratio) NPs (20, 50, 80 wt%) were dispersed well in the mixture of aniline/DBSA under ultrasonic bath for 1 h. 3.28 g APS as initiator was dissolved in 60 mL deionised water and added drop wise to the stirred reaction mixture. Polymerisation was allowed to proceed while stirring in an ice-water bath for 6 h. The nanocomposite was obtained by filtering and washing the suspension with deionised water and ethanol, respectively. The obtained dark-green powder containing (with different weight ratio) $WO_3/MnFe_2O_4$/PANI was dried under vacuum for 24 h.

Results and discussion

The dopant is entrapped via random in the polymer matrix and they have Zwitterion with carbocation on conducting polymers. Therefore incorporation of ferrite and WO_3 do not have effects on doping mechanism. The encapsulation of WO_3 and ferrite materials by PANI is physical method was carried out by nucleation.

XRD data

Figure 1 shows X-ray pattern for the extent of crystallisation of the sensing element in the form of powder. The average crystallite size for the pure WO_3 is 55.66 nm which is calculated from Scherer's formula [24]. XRD pattern shows peaks of hexagonal tungstite. By comparing with the standard XRD pattern of the WO_3 powder, which peaks identified using the ICCD 83–0950 pattern (JCPDS file no. 00-020-1324) with dominant peaks at between 2θ = 20–70 can be attributed to the Miller indices of (001), (020), (200), (120), (-111), (111), (021), (220), (121), (-221), (221), (320), (131), (002), (040), (140), (022), (041), (-401), (-222), (-241), (-132), (150), (250), (042) and (440), respectively. In addition to these peaks, the pattern also manifests presence of large number of peaks of hexagonal tungstite. Figure 2 shows the XRD pattern of $MnFe_2O_4$. According to Figure, cubic ferrite $MnFe_2O_4$ nanoparticles have been obtained. However, there is one peak of α-Fe_2O_3 in the XRD pattern of $MnFe_2O_4$ (2θ = 54) nanoparticles. All peaks correspond to the characteristic peaks of cubic type lattice of $MnFe_2O_4$ (JCPDS file no. 88–1965).

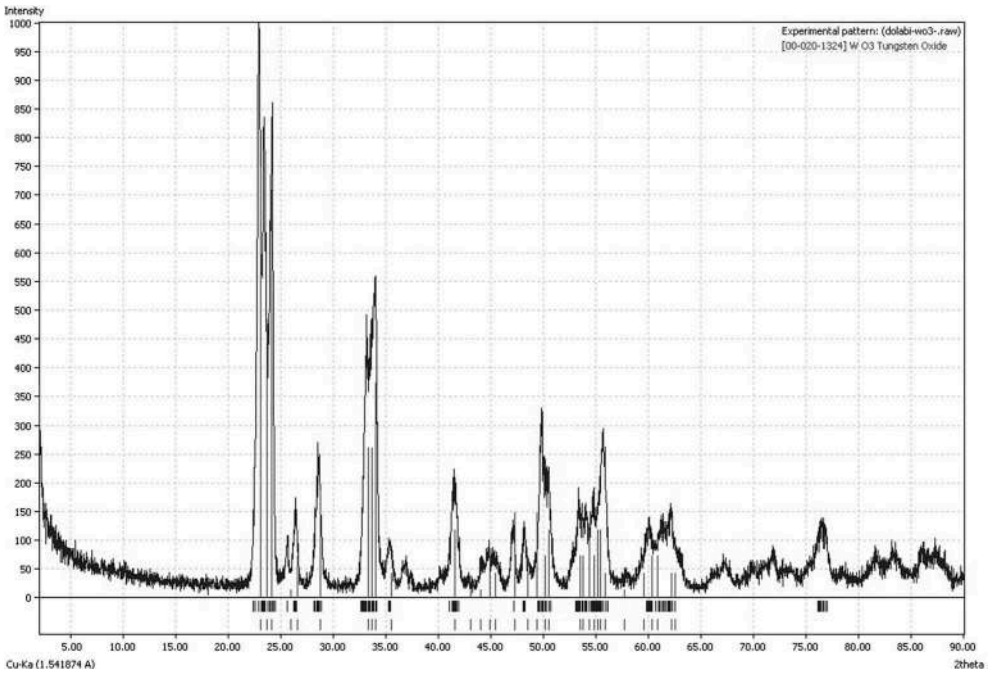

Figure 1. XRD patterns for WO_3 NPs.

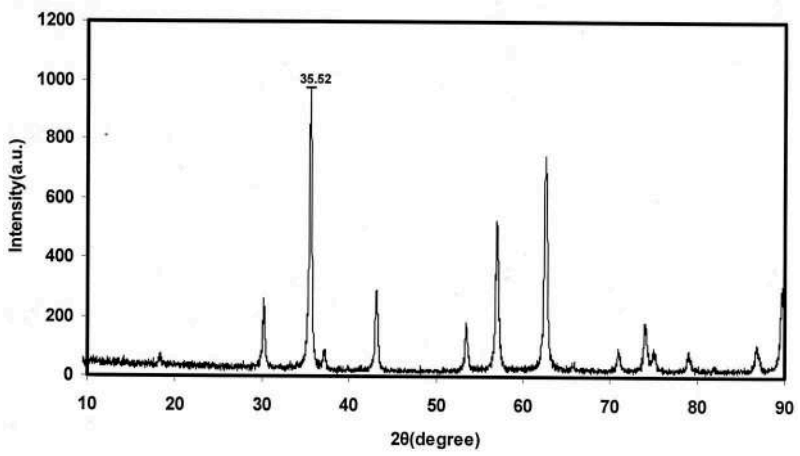

Figure 2. XRD patterns for $MnFe_2O_4$ NPs.

From the obtained peak width of XRD patterns, the size of $MnFe_2O_4$, nanoparticles can be calculated to be 24.27 nm, using the Debye–Scherrer equation.

FTIR spectroscopy

Figure 3(a–c) shows FTIR spectra for (a) WO_3 NPs, (b) $MnFe_2O_3$ NPs and (c) $WO_3/MnFe_2O_3$/PANI nanocomposite (50% wt as core). Figure 3(a) shows an FTIR spectrum for WO_3 NPs, so observed peak at 813 cm^{-1} can be assigned to vibration stretching modes of W-O. The observed wide peak at 570 cm^{-1} in Figure 3(b), can be assigned overlap peaks to vibration stretching modes of Mn-O and Fe-O. FTIR spectrum of $WO_3/MnFe_2O_3$/PANI nanocomposite was showed in Figure 3(c). The specific peak around 1122 cm^{-1} is associated with vibrational modes of N = Q = N (Q refers to the quinonic type rings), indicating that PANI is formed in our sample. The peaks at 1298 and 1238 cm^{-1} are corresponded to N-H bending and asymmetric C-N vibrational stretching of the benzenoid rings, respectively. The peaks at 1473 and 1560 cm^{-1} are attributed to C = N and C = C stretching of the PANI ring (similar to a benzoidal structure). In addition the bands at 2922 and 3429 cm^{-1} are corresponded to the symmetric stretching vibration of C-H aliphatic group of dopant (DBSA) and O-H, N-H stretching modes. According to the mentioned data, it is inferred that the claimed nanocomposite have been successfully synthesised. The observed peaks at 503, 597 and 798 cm^{-1} are attributed to vibration stretching modes of Fe-O, Mn-O in $MnFe_2O_3$ and W-O in WO_3, respectively.

TEM analysis

Figure 4(a-c) shows TEM images of (a) WO_3 NPs, (b) $MnFe_2O_4$ NPs and (c) $WO_3/MnFe_2O_4$/PANI nanocomposite (50% wt as core). The average of WO_3 NPs size is estimated to be 45–50 nm. This particle size is complete agreement with the calculated value with Debye-Scherer formula, which was about 55.66 nm. These particles are polydisperse, and some of them form multi-particle aggregates because of the electro-dipole inter particle interactions. Average particle size of the manganese ferrite powders measured using TEM

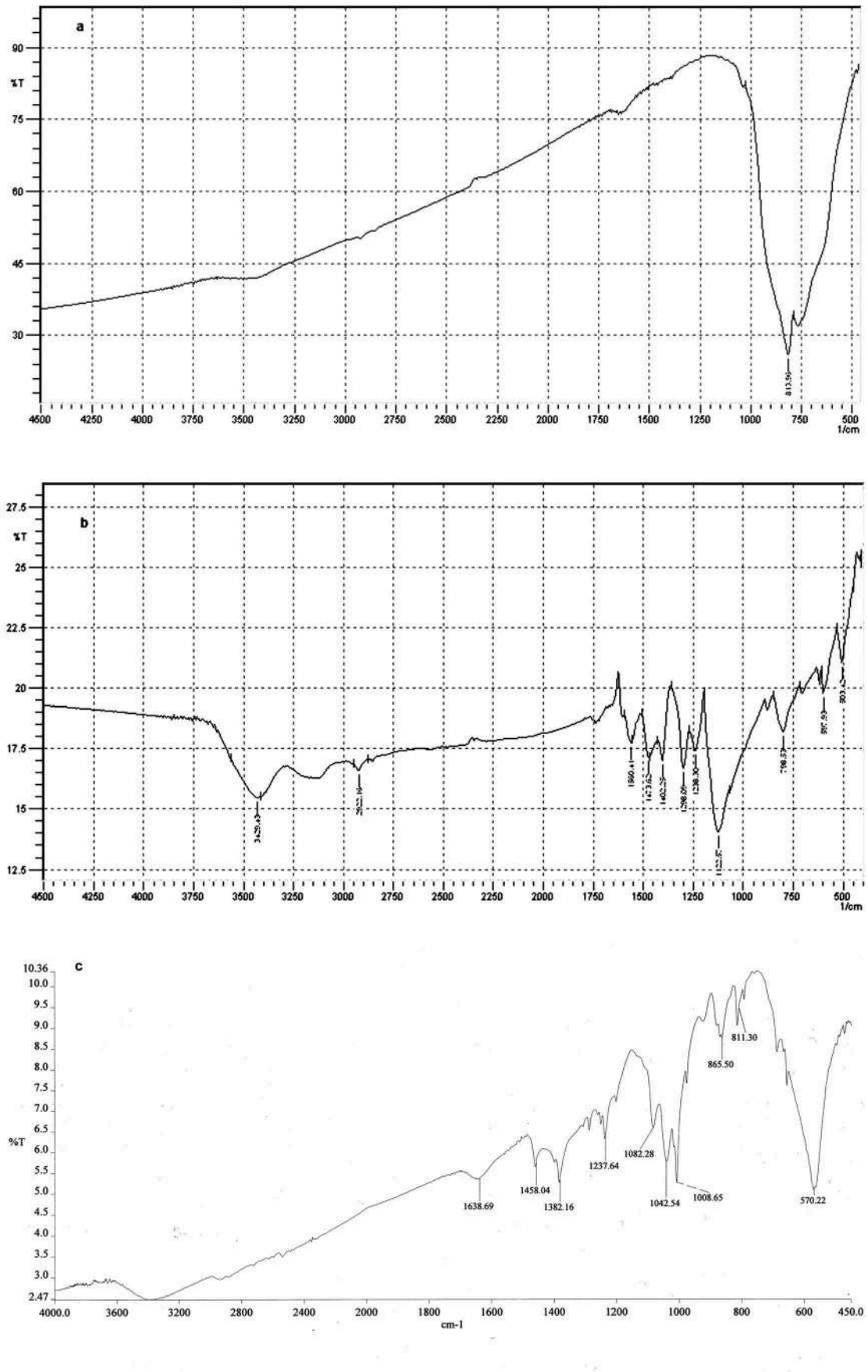

Figure 3. FT-IR spectra for the (a) WO_3 NPs, (b) $MnFe_2O_4$ NPs and (c) $WO_3/MnFe_2O_4$/PANI nanocomposite (50% wt as core).

analysis was shown in Figure 4(b). The photographs indicate that average particle size of the powders was in the 20–30 nm range. Particles were uniformly elongated and formed loose aggregates. This particle size is complete in agreement with the calculated value with Debye-Scherer formula, which was about 24.27 nm, too. Figure 4(c) shows TEM image of $WO_3/MnFe_2O_4$/PANI nanocomposite. It is clear that a PANI coating layer is wrapped around the $WO_3/MnFe_2O_4$ surface,

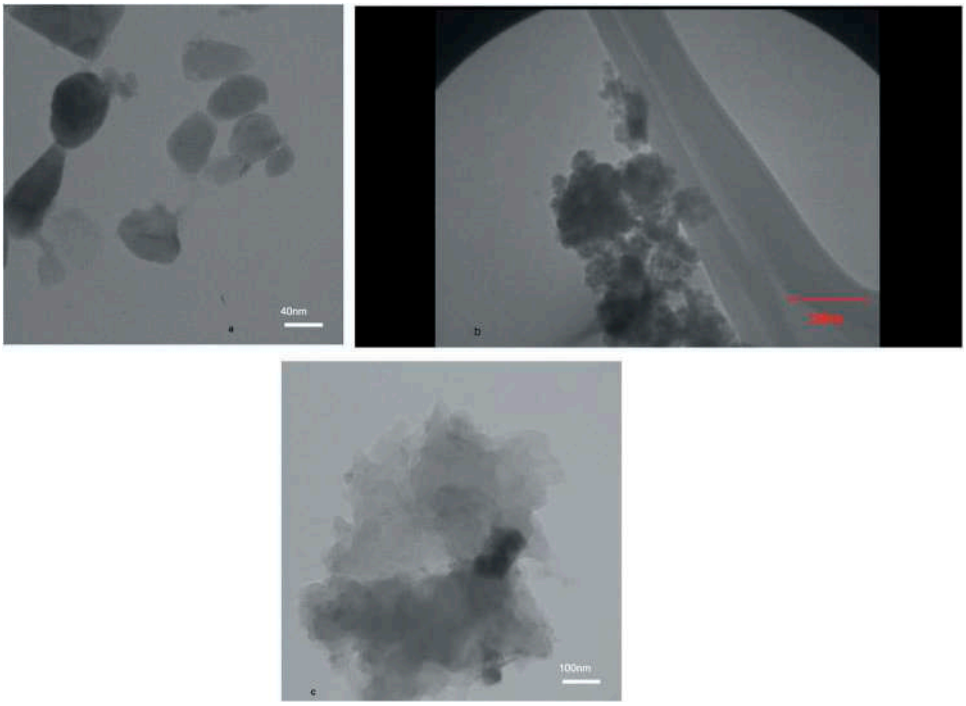

Figure 4. TEM images of the (a) WO_3 NPs, (b) $MnFe_2O_4$ NPs and (c) $WO_3/MnFe_2O_4$/PANI nanocomposite (50% wt as core).

forming a core–shell structure for the $WO_3/MnFe_2O_4$/PANI nanocomposite. The dark region is the magnetic $WO_3/MnFe_2O_4$ as core (70–80 nm) and the grey area is the PANI shell; these colour differences arise because of differing electron penetrability.

SEM images

Figure 5(a–c) shows SEM images of (a) WO_3, (b) $MnFe_2O_4$ and (c) $WO_3/MnFe_2O_4$/PANI nanocomposite (50% wt as core). From the image, it can also be seen that the WO_3 and $MnFe_2O_4$ NPs are about 46 and 25–35 nm. Figure 5(c) shows clearly that the composite was sponge shaped.

Magnetic properties

Magnetic properties of $MnFe_2O_4$ were measured at room temperature with a vibrating sample magnetometer (VSM) at room temperature with an applied field -10 kOe≤H ≤ 10 kOe. Figure 6 show the magnetisation (M) versus the applied magnetic field (H) for $MnFe_2O_4$. The magnetic properties of the ferrite coated PS latex were analysed by room temperature VSM with an above applied field. It can be inferred from the hysteresis loops that all the composite magnetic spheres are magnetically soft at room temperature. The value of saturation magnetisation (M_s) is about 66.7 emu/g, the remnant magnetisation (M_r) and coercivity field are 17.81 emu/g and 110 Oe respectively. VSM of $MnFe_2O_4$ showed ferromagnetic behaviour.

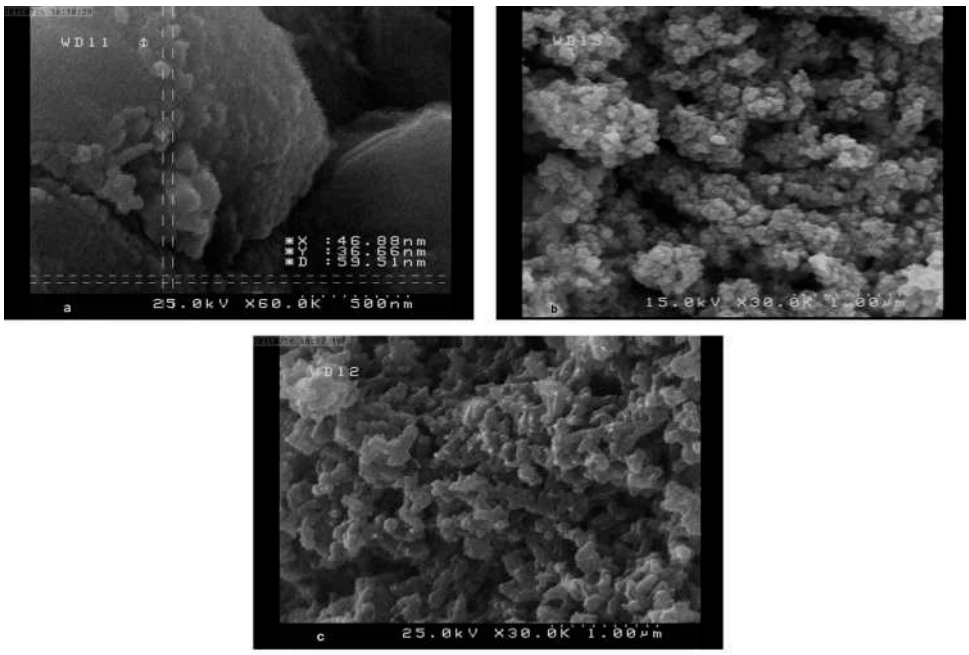

Figure 5. FE-SEM images of (a) WO_3 NPs, (b) $MnFe_2O_4$ NPs and (c) $WO_3/MnFe_2O_4$/PANI nanocomposite (50% wt as core).

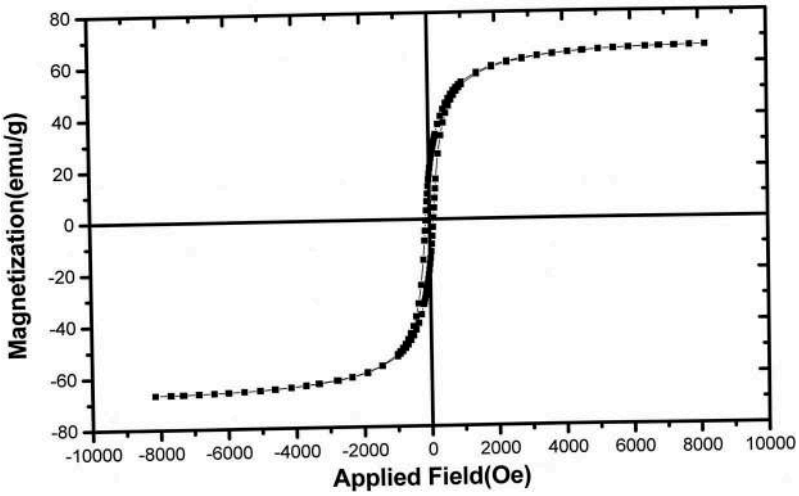

Figure 6. Field-dependent magnetisation curves of $MnFe_2O_4$ NPs.

Conductivity

Electrically conductivity of samples at room temperature was measured by four probe method. The conductivity of PANI after polymerisation by APS as initiator and DBSA as dopant is 0.019 S/cm. When mass content of $WO_3/MnFe_2O_4$ NPs were incorporated, the conductivity of $WO_3/MnFe_2O_4$/PANI nanocomposite with different weight ratios were sharply reduced. The decrease in conductivity of $WO_3/MnFe_2O_4$/PANI nanocomposites, by $WO_3/MnFe_2O_4$ in the core of the NPs may be attributed to the insulting and magnetic behaviours of the ferrite and partial blockage of the conductive path. All conductivities summarised in Table 1.

Thermal infrared absorption study

TIR is a part of the solar spectrum with broad band energy. For TIR application like TIR detectors, thermal imaging, a strong IR absorber operating over the entire wavelength bandwidth is desired. Metal film can be a wide-band absorber for IR radiation with a very small heat capacity, compared with previous designs including intrinsic absorber, black coatings, multilayer absorbers and metal dielectric composite [25]. But polymeric nanocomposites with multi-core shell structure have been reported by our research group [22,23].

On the other hands, TIR tests to be continue on human hand. Human hand have low thermal transmission coefficient and it is suitable for these tests. Figure 7(a–c) shows TIR images for $WO_3/MnFe_2O_4$/PANI nanocomposites in different weight ratio and thickness at (a) without sample, (b) with sample (during of test) and (c) end of test (light reflectivity again) on human hand and summarised in Table 2. Since results of light reflectivity times of samples on human body are lower than $SrTiO_3/BaFe_{12}O_{19}$ [22], but it is suitable for TIR as absorber. The light reflectivity times of samples were increased by increasing weight ratio and thickness. Surface temperature of samples was measured using leaser thermometer after 30 min and summarised in Table 3. The human temperature is 36.7 without sample so, with sample during and end of test, temperature of samples is 34.8. As Table 3 shows, human temperature can not transmit to samples by increasing weight ratio of core. Therefore weight ratio ($WO_3/MnFe_2O_4$ as core) above 60% and 2 mm thickness are the best results as TIR absorber.

Table 1. The electrical conductivity of $WO_3/MnFe_2O_4$/PANI nanocomposites in different weight ratio.

Sample	Conductivity (S/cm)
PANI	0.018
$WO_3/MnFe_2O_4$ 20wt%	5.5×10^{-3}
$WO_3/MnFe_2O_4$ 50wt%	6.3×10^{-5}
$WO_3/MnFe_2O_4$ 80wt%	4.4×10^{-6}

Microwave absorbing study

The difference in microwave absorbing properties of composites are due to the electric loss and magnetic loss generated by the magnetoelectric effects and by the changes of boundary condition of the microwave field at the interface between the polycrystalline $MnFe_2O_4$ NPs and PANI polymer. In this study, we improved magnetoelectric effects and microwave absorbing properties using $WO_3/MnFe_2O_4$/PANI by core-shell structure (50% wt as core). The microwave absorbing properties of the nanocomposite with the coating thickness of 1.5 mm and 13 mm diameter were investigated by using vector network analysers in the frequency range of 8–12 GHz. The results for WO_3, PANI, $MnFe_2O_4$ and $WO_3/MnFe_2O_4$/PANI nanocomposites are shown in Figure 8. Comparison of data for $WO_3/MnFe_2O_4$ and $WO_3/MnFe_2O_4$/PANI reveals that PANI increased the absorption and the electrical conductivity. A minimum reflection loss of WO_3 and $MnFe_2O_4$ NPs were observed -8, -10 dB and -8, -8.2, -10 dB at the frequency of 9.5, 10.5 GHz and 8.7, 10.7, 11.5 GHz, respectively. A minimum reflection loss of $WO_3/MnFe_2O_4$/PANI (50% wt as core) reaches -12, -11, -12 and -11 dB were observed at 8.8, 10.5, 11.6 and 12 GHz, respectively. As seen from Figure 8, the absorption bandwidth under -10 dB are 0 GHz for WO_3, $MnFe_2O_4$, PANI and 2.4 GHz for $WO_3/MnFe_2O_4$/PANI (50% wt as core).

Conclusion

The $WO_3/MnFe_2O_4$/PANI nanocomposites were synthesised with 70–80 nm diameter as TIR and microwave absorbers. The dopant is entrapped via random in the polymer matrix and they have Zwitterion with carbocation on conducting polymers. Therefor incorporation of ferrite and WO_3 don't have effects on doping mechanism. XRD patterns revealed that

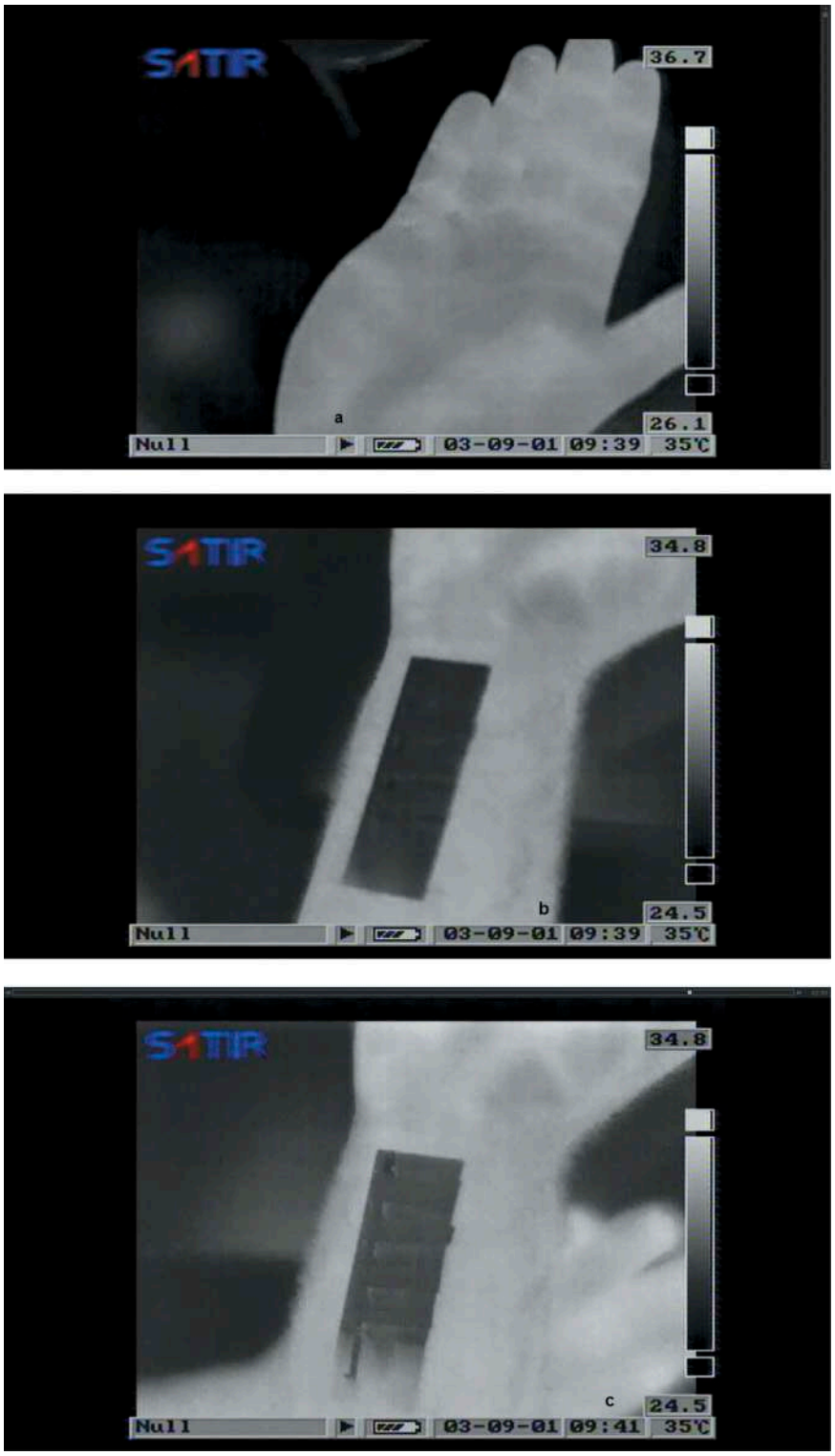

Figure 7. TIR images of $WO_3/MnFe_2O_4$/PANI nanocomposites in different weight ratio and thickness at (a) without sample, (b) with sample (during of test) and (c) end of test (light reflectivity again) on human hand.

Table 2. Relative light reflectivity times (min) again of $WO_3/MnFe_2O_4$/PANI in different weight ratios ($WO_3/MnFe_2O_4$ as core) and thicknesses on human hand.

	Thickness (mm)		
$WO_3/MnFe_2O_4$/PANI (wt% core)	1	1.5	2
20	5	8	12
40	10	14	21
60	15	18	26
80	18	25	35

Table 3. Surface temperature (°C) of $WO_3/MnFe_2O_4$/PANI in different weight ratios ($WO_3/MnFe_2O_4$ as core) and thicknesses on human hand after 30 min (Human temperature; 36.7 °C).

	Thickness (mm)		
$WO_3/MnFe_2O_4$/PANI (wt% core)	1	1.5	2
20	36.1	35.7	35.5
40	35.5	35.0	34.9
60	34.5	34.5	34.4
80	34.0	34.0	33.4

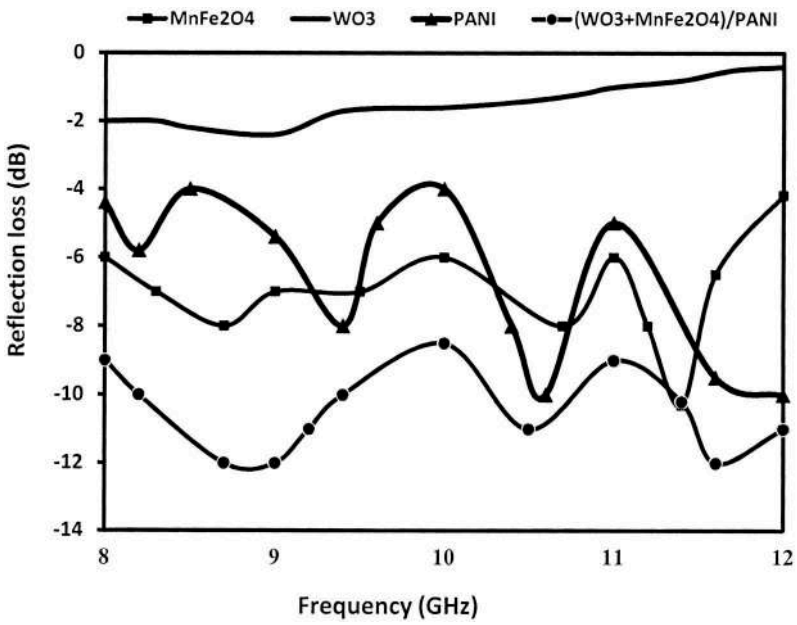

Figure 8. Frequency dependence of minimum reflection loss for the WO_3, $MnFe_2O_4$, PANI and $WO_3/MnFe_2O_4$/PANI nanocomposite (50% wt as core).

$WO_3/MnFe_2O_4$/PANI was formed. In the by core-shell structure, PANI coating on the surface of $WO_3/MnFe_2O_4$ was clearly evident in TEM images. The light reflectivity times of $WO_3/MnFe_2O_4$/PANI nanocomposites on human body were investigated. They are suitable for TIR as absorbers. The light reflectivity times of samples were increased by increasing weight ratio and thickness. Human temperature could not transmit to samples by increasing weight ratio of core. Therefore weight ratio ($WO_3/MnFe_2O_4$ as core) above 60% and 1.5 mm diameter are the best result as TIR absorber. The $WO_3/MnFe_2O_4$/PANI enhanced broad band IR light absorption was observed in the wavelength range of 10–40 μm. The composites powder with 20–80 wt% $WO_3/MnFe_2O_4$ as core possesses good microwave absorption properties. The test microwave absorption properties of the nanoparticles powder dispersing in PANI and thickness of 1.5 mm were investigated using a vector network analysers in the frequency range of 8–12 GHz. A minimum reflection loss of the nanocomposite reaches -12 dB were observed at 8.8 and 11.6 GHz, respectively.

Disclosure statement

No potential conflict of interest was reported by the authors.

Notes on contributors

Mahdi Boujar Dolabi was born 20 September 1983 in Tehran. My Bachelor science was at field applied chemistry from Islamic Azad University, Shareh Ray branch and master science degree at organic chemistry field in Payameh Noor University, Tehran. My research scopes are polymerization on electric and magnetic fields and preparation of IR absorbing materials.

Ali Azimi born 21 August 1991 in Tehran. The period Bachelor at field Applied Chemistry from Islamic Azad University, East Tehran Branch. A masters degree the field of polymer chemistry in Islamic Azad University, East Tehran Branch.Currently a PhD student in Organic Chemistry at Islamic Azad University of Science and Technology in Tehran.

Seyed Hossein Hosseini is full Professor of Organic Chemistry and Polymer Science at Imam Hossein and Islamic Azad Universities, Tehran-Iran. His was born in 10 September 1965. His main research interests cover conducting polymers (synthesis and applications) focus are design of new materials such as toxic gas sensors, conductive liquid crystalline polymers. The recent research activities include electromagnetic absorbing materials such as microwave, thermal IR, UV and laser, X-neutron-gama-ray, and etc. for industry and military applications. He has received numerous awards and he has more than 100 research publications in International journals.

ORCID

Seyed Hossein Hosseini http://orcid.org/0000-0002-1565-6227

References

[1] Xiao-Lin L, Tian-Jun L, Xiao-Ming SYa-Dong L. Highly sensitive wo3 hollow-sphere gas sensors, inorg. Chem. 2004;4317:5442-5449.
[2] Wu Y. Q, Lv G. XLi: S. B. Study of preparation and photo catalytic activity of nanosized wo3 powder. Acta Chim Sinica. 2004;62:1134-1138.
[3] Santos L, Silveira C, Elangovan E, et al. Synthesis of WO 3 nanoparticles for biosensing applications. Sens Actuators B. 2015;223:186–194.
[4] Cheng L. F, Zhang X. T, Chen Y. H, Liu B, Li Y. C, Huang Y. BDu: Z. L. A simple method for synthesizing wo3 nanotubes. Chem J Chin U. 2004;25:162-163.
[5] Pandey NK, Tiwari K, Roy: A. Synthesis and characterization of WO3 nanomaterials. J Biomed Nanotechnol. 2011;7:156–157.
[6] Wang F, Di-Valentin C, Pacchioni G. Doping of WO3for photocatalytic water splitting: hints from density functional theory. J Phys Chem C. 2012;116:8901–8909.
[7] Han B, Popov AL, Shekunova TO, et al. Highly crystalline WO3Nanoparticles are nontoxic to stem cells and cancer cells. J Nanomater. 2019;2019:1–13.
[8] Ghazanfari MR, Kashefi M, Shams SF, et al. Perspective of Fe3O4Nanoparticles role in biomedical applications. Biochem Res Int. 2016;2016:1–32.
[9] Manjunath K, Souza VS, Ganganagappa N, et al. Effect of the magnetic core of (MnFe)2O3@Ta2O5nanoparticles on photocatalytic hydrogen production. New J Chem. 2017;41:326–334.
[10] Hosseini S. H.Asadnia A., Polyaniline/fe3o4 coated on mnfe2o4 nanocomposite. Preparation, Characterization, and

Applications in Microwave Absorption, International Journal Of Physical Sciences. 2013;8(22):1209-1217.
[11] Coltevieille D, Le Méhauté A, Challioui C, et al. Industrial applications of polyaniline. Synth Met. 1999;101:703–704.
[12] Wang Y. Preparation and application of polyaniline nanofibers: an overview. Poly Int. 2018;67:615–769.
[13] Sen T, Mishra S, Shimpi NG. Synthesis and sensing applications of polyaniline nanocomposites: a review. RSC Adv. 2016;6:42196–42222.
[14] Hosseini SH. Study on hard X-ray absorbing properties of nanocluster polyaniline. Mater Sci Semicond Process. 2015;39:90–95.
[15] Kupiec AS, Venkatesan J, AlAnezi AA, et al. Magnetic nanomaterials and sensors for biological detection. Nanomed. 2016;12:2459–2473.
[16] Hosseini SH, Asadnia A, Moloudi: M. Preparation and electromagnetic wave absorption hard–soft Ba ferrite/polypyrrole core–shell nanocomposites. Mater Res Innovations. 2015;19:107–112.
[17] Hosseini SH, Alamian A, Mousavi SM. Preparation of magnetic and conductive graphite nanoflakes/SrFe12O19/polythiophene nanofiber-nanocomposites and its radar absorbing application. Fibers Polym. 2016;17:593–599.
[18] Suarez A, Victoria J, Alcarria A, et al. Investigation on the thermal behavior, mechanical properties and reaction characteristics of Al-PTFE composites enhanced by Ni particle. Materials (Basel). 2018;11(2):E174, 1–20.
[19] Hosseini SH, Moghimi A, Moloudi M. Magnetic, conductive, and microwave absorption properties of polythiophene nanofibers layered on MnFe2O4/Fe3O4 core–shell structures. Mater Sci Semicond Process. 2014;24C:272–277.
[20] Hosseini SH, Soltanabadi Z. Investigation of X-ray shielding properties of Au nano-composite-based polyaniline. Mater Res Innovation. 2016;20:300–306.
[21] Yang CC, Gung YJ, Hung WC, et al. Infrared and microwave absorbing properties of BaTiO3/polyaniline and BaFe12O19/polyaniline composites. Compos Sci Technol. 2010;70:466–471.
[22] Hosseini SH, Zamani P, Mousavi SY. Thermal infrared and microwave absorbing properties of SrTiO 3 /SrFe 12 O 19 /polyaniline nanocomposites. J Alloys Compd. 2015;644:423–429.
[23] Hosseini SH, Zamani: P. Preparation of thermal infrared and microwave absorber using SrTiO3/BaFe12O19/polyaniline nanocomposites. J Magn Magn Mater. 2016;397:205–212.
[24] Langford JI, Wilson AJC. Scherrer after sixty years. J Appl Cryst. 1978;11:102–113.
[25] Granqvist CG. Solar energy materials. Adv Mater (Deerfield Beach Fla). 2003;15:1789–1803.